Osteoconductivity of strontium-doped bioactive glass particles: A histomorphometric study in rats

Alejandro A. Gorustovich,[1,2] Tammy Steimetz,[3] Rómulo L. Cabrini,[3] José M. Porto López[2,4]
[1]*Research Laboratory, National Atomic Energy Commission (CNEA-Regional Noroeste), Salta A4408FTV, Argentina*
[2]*National Research Council (CONICET), C1033AAW Buenos Aires, Argentina*
[3]*Department of Oral Pathology, School of Dentistry, University of Buenos Aires, Buenos Aires, C1122AAH, Argentina*
[4]*Ceramics Division, Research Institute for Materials Science and Technology (INTEMA-CONICET), Mar del Plata B7608FDQ, Argentina*

Received 20 November 2007; revised 29 July 2008; accepted 15 October 2008
Published online 26 January 2009 in Wiley InterScience (www.interscience.wiley.com). DOI: 10.1002/jbm.a.32355

Abstract: There is accumulating evidence that strontium (Sr)-containing bioceramics have positive effects on bone tissue repair. The aims of the present study were to evaluate the osteoconductivity of Sr-doped bioactive glass (BG) particles implanted in rat tibia bone marrow, and characterize the neoformed bone tissue by SEM-energy-dispersive X-ray microanalysis. Melt-derived BGs were prepared from a base 45S5 BG. Sr-doped glass (45S5.6Sr) was prepared using 6 wt % SrO as a substitute for the CaO. Histological analysis using undecalcified sections showed that new lamellar bone had formed along the surface of both 45S5 and 45S5.6Sr BG particles within 4 weeks. To evaluate osteoconductivity, affinity indices were calculated. At 30 days after implantation, 45S5 and 45S5.6Sr BGs had almost identical affinity indices (88% ± 7% and 87% ± 9%; $p > 0.05$). Strontium was not detected in the neoformed bone tissue surrounding 45S5.6Sr BG particles. These results indicate that 45S5.6Sr BG particles are osteoconductive when implanted inside the intramedullary canal of rat tibiae, and no alterations in bone mineralization, in terms of Ca/P ratio, were observed in the neoformed bone tissue around 45S5.6Sr BG particles. © 2009 Wiley Periodicals, Inc. J Biomed Mater Res 92A: 232–237, 2010

Key words: osteoconductivity; affinity index; bioactive glass; strontium; bone

INTRODUCTION

Because of their positive effects on bone biology, the incorporation of strontium (Sr) in the calcium phosphate ceramics and cements for bone tissue repair has been a subject of great interest in the last decade.[1–16] It has been shown that Sr-containing calcium phosphate ceramics promoted better osteoprecursor cell attachment and proliferation and showed no deleterious effects on osteoblast cell adhesion, extracellular matrix formation, and mineralization *in vitro*.[4,7,12,14,16] Several studies show that the Sr-containing hydroxyapatite (Sr-HA) bioactive bone cement promotes osteoblast attachment and mineralization *in vitro* and bone growth and osseointegration *in vivo*.[2,3,8–12]

Bioactive glasses (BGs) or glass-ceramics have been the subjects of intensive research in view of their stimulatory effect on bone tissue formation. To the best of our knowledge, the studies that have examined the effect of incorporating Sr to vitreous bioceramics have used physicochemical and structural properties of the materials as end-points.[17–22] However, the *in vitro* or *in vivo* bone behavior of glass or glass-ceramics modified by Sr have not been evaluated to date. Thus, the aim of the present study was to perform a histological and histomorphometric evaluation of osteoconductivity of Sr-doped BG particles implanted in rat tibia bone marrow. Sr is known to be incorporated into the crystal lattice of hydroxyapatite, thus it was of interest to determine Sr content at the bone-BG interface and the newly formed bone tissue around BG particles by X-ray microanalysis.

Correspondence to: A. A. Gorustovich; e-mail: alegorustov@ciudad.com.ar

Contract grant sponsor: National Agency for the Promotion of Science and Technology (ANPCyT); contract grant number: PICT 05-11870

MATERIALS AND METHODS

Bioactive glasses

Melt-derived glasses (45S5 and 45S5.6Sr) were prepared from a base 45S5 BG. Sr-doped glass (45S5.6Sr) was prepared using 6 wt % SrO as a substitute for the CaO in 45S5 BG. The compositions of the glasses are given in Table I.

The raw materials (quartz > 99% SiO_2, $CaCO_3$, Na_2CO_3, $CaHPO_4{\cdot}2H_2O$, and $SrCO_3$) were mixed in the desired stoichiometries, and melted in an electrical furnace (Carbolite RHF 17/6S, Carbolite Ltd, England) for 3 h at 1350°C. A platinum crucible was used to avoid contamination of the melt. After the melting process, the glasses were cast into a graphite mold, crushed, and sieved to 300–350 μm particles. Differential thermal analysis (DTA) and X-ray diffraction (XRD) of the prepared glasses were performed.

DTA of glass samples was carried out at a heating rate of 10°C/min with a Shimadzu DTA-50H station under N_2 purge (40 mL/min). XRD analysis was performed with a Philips PW1830 diffractometer (Co Kα radiation).The instrument was operated at 40 kV and 30 mA.

Animals

Male Wistar rats (n = 15) (International Laboratory Code Registry: Hsd:Wi-ffyb) weighing 100 ± 20 g were used throughout. The animals were not given a special diet. They were fed rat chow and given water *ad libitum,* housed in steel-cages and maintained on a 12:12 hour light dark cycle. The guidelines of the National Institutes of Health for the care and use of laboratory animals (NIH Publication No. 85–23, Rev. 1985) were observed. The protocol was examined and approved by the institutional ethics committee of the School of Dentistry, University of Buenos Aires.

Surgical procedure

All the animals were anesthetized by intraperitoneal administration of a 4:1 solution of ketamine/xylazine, that is, ketamine chlorhydrate, 50 mg/mL (Ketamina 50® Holliday-Scott, Buenos Aires, Argentina) and xylazine, 20 mg/mL (Rompun® Bayer, Buenos Aires, Argentina) at a dose of 0.15 mL per 100 g body weight. The skin was disinfected and shaved. A longitudinal 1.5-cm incision was made along the frontal aspect of both tibiae. The subcutaneous tissue, muscles, and ligaments were dissected to expose the external surface of the tibiae in the area of the diaphyseal bone. An end-cutting bur (1.5 mm in diameter) was used to drill a hole reaching the bone marrow. Overheating and additional bone damage were prevented by using manual rotating impulsion.[23] 45S5 BG particles (15 mg) were placed inside the medullary compartment of the tibia (45S5 group), while in the contralateral tibia, 15 mg of 45S5.6Sr BG particles were implanted (45S5.6Sr group). The wounds were carefully sutured with an absorbable polyglactin 910 suture (Vicryl, Ethicon Inc., USA). The animals were sacrificed 30 days after implantation by an intraperitoneally administered overdose of sodium pentobarbital. The tibiae were resected, fixed in 20% formalin solution, cleaned of soft tissue, and radiographed.

TABLE I
Compositions of Glasses in Weight Percent

Glass	SiO_2	CaO	SrO	Na_2O	P_2O_5
45S5	45	24.5	0	24.5	6
45S5.6Sr	45	18.5	6	24.5	6

Histologic processing

The undecalcified tibiae were processed for embedding in methyl-methacrylate resin. The samples were then sectioned using a diamond saw (Exakt Apparatebau, Germany) and three slices were cut at ~500 μm, perpendicular to the major axis of the tibiae; that is, in the middle of the implant bed and two points equidistant from the middle. The cross sections were ground using a grinding machine (Exakt Apparatebau, Germany) and finished manually with sandpaper to obtain sections of about 35 μm thick. The sections were stained with 1% toluidine blue for histologic and histomorphometric evaluation by light microscopy (Zeiss Axioskop 2 MOT, Carl Zeiss, Jena, Germany). Then, two specimens were carbon-coated in a vacuum evaporator (CAR 001-0045) for energy dispersive X-ray analysis (EDX).

Histomorphometry

The percentage of bone-implant contact (affinity index) of the BGs were evaluated quantitatively, as described elsewhere.[24] The affinity index, which equaled the length of bone in direct contact with the BG particles surface expressed as a percentage of the total length of the BG particles surface, was calculated for each BG at 30 days after implantation.

X-ray microanalysis

To determine the whole line profile through the bone-interface-BG, the sections were examined in a scanning electron microscope (JEOL JSM 6480 LV, Japan) equipped with EDX system (Thermo Electron, NORAM System SIX NSS-100) in keeping with a previously described technique.[25] The relative amounts of silicon (Si Kα), strontium (Sr Lα), calcium (Ca Kα), and phosphorus (P Kα) elements were mainly analyzed at a voltage of 15 kV. The Sr Kα was also been analyzed; however, a voltage of 30 kV was required. The Ca/P ratio was determined at the bone-BG interface and the bone tissue around BG particles.

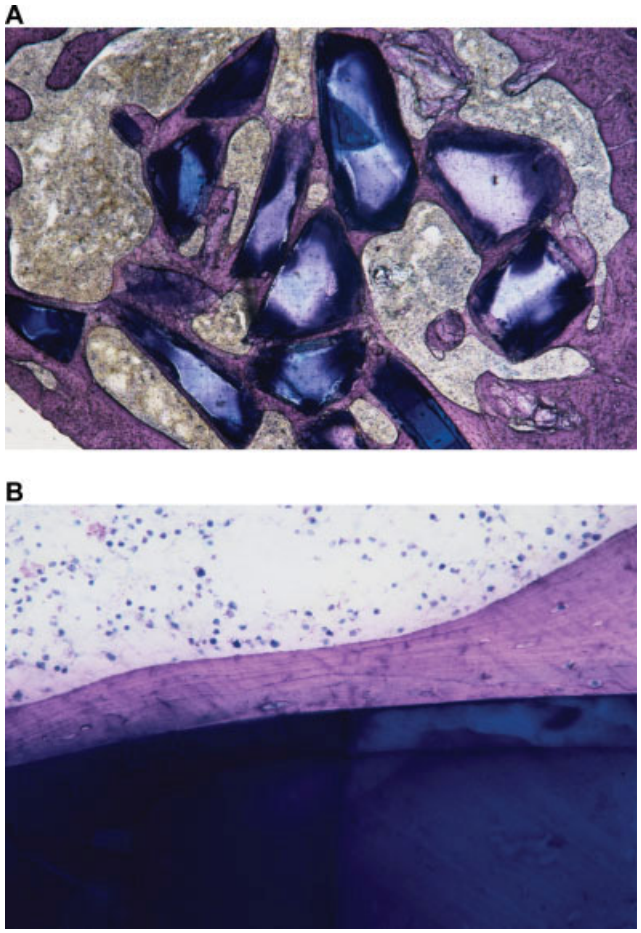

Figure 1. Undecalcified ground sections. Thirty days postimplantation; (A) Note the neoformed bone tissue around the 45S5.6Sr particles, (B) observation at high-power magnification evidenced bone tissue in close contact with the 45S5.6Sr BG surface (toluidine blue; original magnification ×50 (A), ×200 (B).

Statistical analysis

The results were statistically analyzed by Student's *t*-test. Data were reported as mean ± SD. The level of statistical significance was set at $p < 0.05$.

RESULTS

Characterization of materials

The XRD patterns of the as-cast glasses show the noncrystalline nature of the obtained solid, as a consequence of the rapid cooling from the melt (data not shown).

The DTA curve of 45S5 glass depicted an exothermal peak corresponding to glass crystallization at 690°C. 45S5.6Sr glass showed two exothermal events, that is, one at 810°C and another at 850°C. In addition, the 45S5 and 45S5.6Sr glass samples were heated at 900°C for 24 h to induce complete crystallization. In each case, the crystalline phases were identified by XRD analysis. All the peaks observed in 45S5 glass samples corresponded to the $Na_2Ca_2Si_3O_9$ phase, a compound associated to the area of primary crystallization of glass. However, 45S5.6Sr glass had $Na_2Ca_2Si_3O_9$ as a major phase as well as some unidentified phases.

In vivo bioactivity

Uncomplicated healing after implantation in all rats was observed. All implants remained *in situ* as determined by radiographs.

Microscopic findings

Light microscopy of the histologic sections at 30 days after implantation showed that an intimate contact between the surface of both BGs and lamellar bone without any intervening fibrous layer was widespread [Fig. 1(A,B)]. There was no occurrence of macrophages or related inflammatory cells in any of the interface regions of either of the groups.

Histomorphometric analysis

The affinity indices of 45S5 and 45S5.6Sr BGs 30 days after implantation were 88% ± 7% and 87% ± 9%, respectively. There were no significant differences between the affinity indices of the two BGs examined (Fig. 2) ($p > 0.05$).

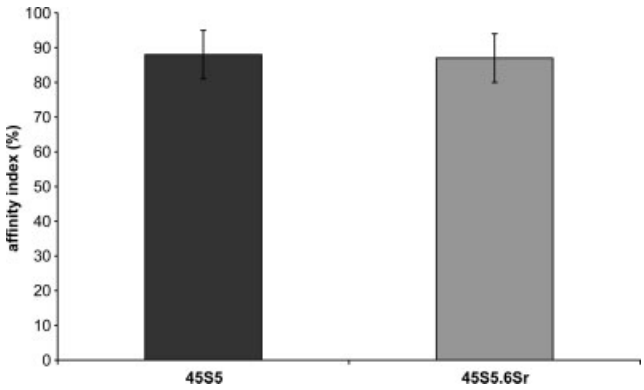

Figure 2. Affinity indices of 45S5 and 45S5.6Sr BGs particles 30 days after implantation in rat tibiae.

X-ray microanalysis

Bone-BG interface

EDX analysis showed calcium (Ca, 50 ± 8 at%) and phosphorus (P, 33 ± 5 at%) contents at the bone-BG interface in the 45S5 group. Besides Ca (54 ± 7 at%) and P (34 ± 3 at%), strontium (Sr Kα) (1.24 ± 0.18 at%) was also detected at the bone-BG interface in the 45S5.6Sr group (Fig. 3). The Ca/P ratio for the 45S5.6Sr group (1.60 ± 0.14) did not differ significantly from the value seen for the 45S5 group (1.57 ± 0.10) ($p > 0.05$).

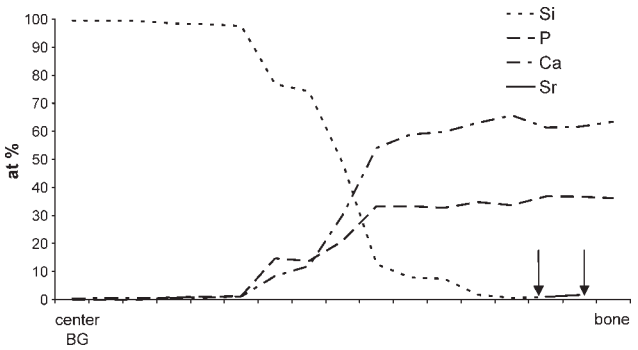

Figure 3. Line-scan EDX through the bone-interface-BG (45S5.6Sr). Strontium content is clearly seen at the Ca-P-rich layer at the interface (between arrows).

Newly formed bone

EDX analysis of the newly formed bone at 30 days after implantation revealed that the contents of Ca and P for the 45S5.6Sr group (60 ± 0.87; 40 ± 0.87 at%) did not differ significantly from the values seen for the 45S5 group (60 ± 0.90; 40 ± 0.90 at%), respectively ($p > 0.05$). Strontium was not detected in the neoformed bone tissue surrounding 45S5.6Sr BG particles at 30 days after implantation (Fig. 3). The Ca/P ratio of bone tissue for the 45S5.6Sr group (1.51 ± 0.04) did not differ significantly from the value seen for the 45S5 group (1.51 ± 0.06) ($p > 0.05$).

DISCUSSION

There is growing evidence that strontium (Sr) influences bone cells and bone metabolism *in vitro* and *in vivo*.[26] For the first time, this study describes the *in vivo* bone response to the Sr-containing BG particles in the SiO_2-CaO-Na_2O-P_2O_5 system implanted in rat tibia bone marrow. The results of the present study provide evidence that there were no significant differences among the osteoconductive potentials of 45S5 and 45S5.6Sr BG particles. As such, osseointegration of bone and the both BGs was achieved.

It has been well established that the percentage of bone at the material-tissue interface, the affinity index, is a reasonable parameter to use for the quantitative comparison of the osteoconductive potentials of different biomaterials.[24] However, there are few reports about quantitative analysis of the osteoconductive potential of Sr-containing bioceramics, by determining their affinity indices. Wong et al. investigated the *in vivo* bone response to the Sr-containing hydroxyapatite (Sr-HA) bioactive bone cement injected into the cancellous bone of the iliac crest of rabbits for 1, 3, and 6 months.[2] The formation of an osteoid layer and osteoblast adhesion was evidence of new bone formation 1 month after implantation. Newly formed bone was observed to grow onto the bone cement after 3 months. The affinity of bone on Sr-HA cement was increased from 73.55% ± 3.50% after 3 months up to 85.15% ± 2.74% after 6 months.[2] Ni et al. evaluated the Sr-HA bone cement in primary hip replacement using a rabbit model. The overall affinity index of bone on Sr-HA cement was 85% ± 5% 6 months after implantation.[8]

In our study, there were no significant differences between the affinity indices of each BGs examined. The overall affinity index of bone on both 45S5 and 45S5.6Sr BG particles was ~88% as early as 30 days after implantation, similar to the results obtained by Ono et al. and Ikeda et al. using apatite-and wollastonite-containing glass-ceramic (A-W GC) granules who reported that 89% of the surface of dense A-W GC granules were covered with newly formed bone within 4 weeks of their implantation into rat tibiae.[24,27] However, our results indicated that 45S5 BG had higher affinity index (88% ± 7%) than 45SS BG particles implanted in the distal femoral epiphysis of rabbits as reported by Vogel et al. (30–60%; 28 days after implantation).[28] These differences in bone bonding capabilities usually are attributed to the different animal implantation model, particle size, and the ratio of implant surface to implantation site volume.[29]

Energy-dispersive X-ray (EDX) analysis revealed that both 45S5 and 45S5.6Sr BG particles bonded to bone through a calcium-phosphorus interface. Results of this study were consistent with previous studies showing that surface bioactive ceramics bond to bone through an apatite layer.[2,3,8–10,13,24,27] It is noteworthy that the Sr content (1.24 ± 0.18 at%) detected at the bone-BG interface in the 45S5.6Sr group did not alter their osteoconductivity, that is, *in vivo* bioactivity as compared with 45S5 BG.

In the present study, Sr was not detected in the bone tissue surrounding 45S5.6Sr BG particles at

30 days after implantation. However, our previous studies showed the presence of Sr (1.05 ± 0.24 at%) in the newly formed bone surrounding 45S5.6Sr BG particles at 15 days after implantation. This occurred without any modification in the ratio Ca/P (unpublished data).

Recently, the changes in chemical composition, crystal size, crystallinity, and lattice structure of apatite after synthetic incorporation of Sr were evaluated by Li et al. to gain insight into bone crystal changes after incorporation of Sr. Sr-substituted hydroxyapatite nanocrystallite with different Sr content were synthesized.[30] The XRD and transmission electron microscopy (TEM) results indicated that the Sr incorporation at atomic ratio lower than 1.5% did not impact the chemical composition and crystal structure while increased the crystal size slightly. However, 15% Sr incorporation dramatically decreased the crystal size and crystallinity.[30] Thus, changes at the bone crystal level must be evaluated in further studies using Sr-containing biomaterials.

CONCLUSION

Results suggested good bone-bonding ability of the 45S5.6Sr BG particles when implanted into the intramedullary canal of rat tibiae. In addition, a preservation of the normal bone mineralization, in terms of Ca/P ratio was observed in the neoformed bone tissue around 45S5.6Sr BG particles, making the use of the Sr-containing silica-based BGs a potential alternative in bone tissue engineering and regenerative medicine procedures.

The authors gratefully acknowledge the expert assistance of Pedro Villagrán, Ch.E., and Silvia Blanco, Ch.E. with SEM-EDX, LASEM-ANPCyT-UNSa-CONICET, Salta, Argentina.

References

1. Li YW, Leong CY, Lu WW, Luk DK, Cheung KMC, Chiu KY, Chow SP. A novel injectable bioactive bone cement for spinal surgery: A developmental and preclinical study. J Biomed Mater Res 2000;52:164–170.
2. Wong CT, Lu WW, Chan WK, Cheung KM, Luk KD, Lu DS, Rabie AB, Deng LF, Leong JC. In vivo cancellous bone remodeling on a strontium-containing hydroxyapatite (Sr-HA) bioactive cement. J Biomed Mater Res A 2004;68:513–521.
3. Wong CT, Chen QZ, Lu WW, Leong JC, Chan WK, Cheung KM, Luk KD. Ultrastructural study of mineralization of a strontium-containing hydroxyapatite (Sr-HA) cement in vivo. J Biomed Mater Res A 2004;70:428–435.
4. Kim HW, Koh YH, Kong YM, Kang JG, Kim HE. Strontium substituted calcium phosphate biphasic ceramics obtained by a powder precipitation method. J Mater Sci Mater Med 2004; 15:1129–1134.
5. Saint-Jean SJ, Camiré CL, Nevsten P, Hansen S, Ginebra MP. Study of the reactivity and in vitro bioactivity of Sr-substituted alpha-TCP cements. J Mater Sci Mater Med 2005;16: 993–1001.
6. Guo D, Xu K, Zhao X, Han Y. Development of a strontium-containing hydroxyapatite bone cement. Biomaterials 2005;26: 4073–4083.
7. Qiu K, Zhao XJ, Wan CX, Zhao CS, Chen YW. Effect of strontium ions on the growth of ROS17/2.8 cells on porous calcium polyphosphate scaffolds. Biomaterials 2006;27:1277–1286.
8. Ni GX, Lu WW, Chiu KY, Li ZY, Fong DY, Luk KD. Strontium-containing hydroxyapatite (Sr-HA) bioactive cement for primary hip replacement: An in vivo study. J Biomed Mater Res B Appl Biomater 2006;77:409–415.
9. Ni GX, Chiu KY, Lu WW, Wang Y, Zhang YG, Hao LB, Li ZY, Lam WM, Lu SB, Luk KD. Strontium-containing hydroxyapatite bioactive bone cement in revision hip arthroplasty. Biomaterials 2006;27:4348–4355.
10. Ni GX, Lu WW, Xu B, Chiu KY, Yang C, Li ZY, Lam WM, Luk KD. Interfacial behaviour of strontium-containing hydroxyapatite cement with cancellous and cortical bone. Biomaterials 2006;27:5127–5133.
11. Ni GX, Lu WW, Tang B, Ngan AH, Chiu KY, Cheung KM, Li ZY, Luk KD. Effect of weight-bearing on bone-bonding behavior of strontium-containing hydroxyapatite bone cement. J Biomed Mater Res A 2007;83:570–576.
12. Li ZY, Yang C, Lu WW, Xu B, Lam WM, Ni GX, Abbah SA, Yang F, Cheung KM, Luk KD. Characteristics and mechanical properties of acrylolpamidronate-treated strontium containing bioactive bone cement. J Biomed Mater Res B Appl Biomater 2007;83:464–471.
13. Oliveira AL, Reis RL, Li P. Strontium-substituted apatite coating grown on Ti6Al4V substrate through biomimetic synthesis. J Biomed Mater Res B Appl Biomater 2007;83:258–265.
14. Panzavolta S, Torricelli P, Sturba L, Bracci B, Giardino R, Bigi A. Setting properties and in vitro bioactivity of strontium-enriched gelatin-calcium phosphate bone cements. J Biomed Mater Res A 2007;84:965–972.
15. Landi E, Tampieri A, Celotti G, Sprio S, Sandri M, Logroscino G. Sr-substituted hydroxyapatites for osteoporotic bone replacement. Acta Biomater 2007;3:961–969.
16. Wu C, Ramaswamy Y, Kwik D, Zreiqat H. The effect of strontium incorporation into $CaSiO_3$ ceramics on their physical and biological properties. Biomaterials 2007;28:3171–3181.
17. Galliano PG, Porto López JM, Varetti EL, Sobrados I, Sanz J. Analysis by nuclear magnetic resonance and raman spectroscopies of the structure of bioactive alkaline-earth silicophosphate glasses. Mater Res Bull 1994;29:1297–1306.
18. Galliano PG, Cavalieri AL, Porto López JM. A study by density measurements and indentation tests of a calcium silicophosphate bioactive glass with different MgO or SrO contents. J Non-Cryst Solids 1995;191:311–320.
19. Galliano PG, Porto López JM. Termal behaviour of bioactive alkaline-earth silicophosphate glasses. J Mater Sci Mater Med 1995;6:353–359.
20. Hill RG, Stamboulis A, Law RV, Clifford A, Towler MR, Crowley C. The influence of strontium substitution in fluorapatite glasses and glass-ceramics. J Non-Cryst Solids 2004; 336:223–229.
21. Pires R, Abrahams I, Nunes TG, Hawkes GE. Non-random cation distribution in sodium-strontium-phosphate glasses. J Non-Cryst Solids 2004;337:1–8.
22. Keding R, Rüssel C. Oriented strontium fresnoite glass-ceramics prepared by electro-chemically induced nucleation. J Mater Sci 2004;39:1433–1435.
23. Gorustovich AA, Sivak MG, Guglielmotti MB. A novel methodology for imaging new bone formation around bioceramic bone substitutes. J Biomed Mater Res A 2007;8:443–445.

24. Ikeda N, Kawanabe K, Nakamura T. Quantitative comparison of osteoconduction of porous, dense A-W glass-ceramic and hydroxyapatite granules (effects of granule and pore sizes). Biomaterials 1999;20:1087–1095.
25. Huygh A, Schepers EJG, Barbier L, Ducheyne P. Microchemical transformation of bioactive glass particles of narrow size range, a 0–24 months study. J Mater Sci Mater Med 2002;13:315–320.
26. Marie PJ, Ammann P, Boivin G, Rey C. Mechanisms of action and therapeutic potential of strontium in bone. Calcif Tissue Int 2001;69:121–129.
27. Ono K, Yamamuro T, Nakamura T, Kokubo T. Quantitative study on osteoconduction of apatite-wollastonite containing glass ceramic granules, hydroxyapatite granules, and alumina granules. Biomaterials 1990;11:265–271.
28. Vogel M, Voigt C, Gross UM, Müller-Mai CM. In vivo comparison of bioactive glass particles in rabbits. Biomaterials 2001;22:357–362.
29. Ducheyne P. Effect of bioactive glass particle size on osseous regeneration. J Biomed Mater Res 1999;46:301–304.
30. Li ZY, Lam WM, Yang C, Xu B, Ni GX, Abbah SA, Cheung KM, Luk KD, Lu WW. Chemical composition, crystal size and lattice structural changes after incorporation of strontium into biomimetic apatite. Biomaterials 2007;28:1452–1460.